


Cite this: *RSC Adv.*, 2019, 9, 39811

# Phosphorus removal and mechanisms by Zn-layered double hydroxide (Zn-LDHs)-modified zeolite substrates in a constructed rapid infiltration system†

Xiangling Zhang,\* Jingtian Gao, Yu Lei,  Zhouying Xu, Shibin Xia,\* Yinghe Jiang and Jing Cheng

This work presents novel materials, ZnFe-LDHs-modified ( $\text{Zn}^{2+} : \text{Fe}^{3+}$  molar ratio of 2 : 1 and 3 : 1) and ZnAl-LDHs-modified ( $\text{Zn}^{2+} : \text{Al}^{3+}$  molar ratio of 2 : 1 and 3 : 1) zeolites, which were synthesized under alkaline conditions *via* a co-precipitation method and coated *in situ* on original zeolites. The as-prepared LDHs-modified zeolites were used as substrates for a constructed rapid infiltration system (CRIS) to conduct purification experiments to investigate the phosphorus removal performance of all types of zeolites. The experimental results showed that the phosphorus removal rates of the Zn-LDHs-modified zeolites reached over 80%, which are superior to that of the original zeolites. Furthermore, isothermal adsorption and adsorption kinetic experiments were conducted to explore the adsorption mechanisms. The theoretical maximum adsorption capacities were efficiently enhanced owing to the Zn-LDHs coating strategy. Especially, that of the ZnFe-LDHs-modified (3 : 1) zeolites reached 434.78  $\text{mg kg}^{-1}$ , which is much higher than that of the original zeolites. Meanwhile, according to the fitting results of the adsorption kinetics experiments, it was found that the predominant adsorption type of the original zeolites was converted from intrinsically weak physical adsorption into more stable chemical adsorption by the Zn-LDHs coating. Furthermore, high-throughput sequencing was also exerted to uncover the phosphorus removal mechanism by microorganisms. The obtained results indicate that the relative abundance of *Pseudomonas* and *Dechloromonas*, which are closely related to phosphorus removal, effectively increased. Overall, the Zn-LDHs-modified zeolites improved the phosphorus removal performance efficiently and sustainably when applied in CRIS.

Received 26th June 2019

Accepted 11th November 2019

DOI: 10.1039/c9ra04826j

rsc.li/rsc-advances

## Introduction

A large amount of phosphorus is discharged into natural water body as diluted waste, which often leads to pollution of the water environment.<sup>1</sup> Domestic and industrial wastewater discharge, especially from point sources, significantly endanger aquatic water quality.<sup>2</sup> Excess phosphorus discharged from domestic, agricultural, and industrial sources to surface water causes serious water pollution problems and is an essential factor for eutrophication.<sup>3</sup> Anthropogenic activities have greatly accelerated the rate at which nutrients enter the ecosystem in the past decades.<sup>4</sup> Therefore, it is necessary to develop new methods for the simultaneous removal of these nutrients to prevent eutrophication.<sup>5</sup> Nowadays, various physical, chemical and biological methods have been proposed to reduce

phosphorus in sewage discharge.<sup>6–11</sup> Among them, chemical precipitation with iron or alum in various reactors is most commonly used, but this produces large amounts of sludge, which must be properly disposed.<sup>7,10,11</sup> Bioremediation of phosphorus containing wastewater has been proven to be the most eco-friendly method, but plant harvest and disposal must be considered.<sup>8</sup> Electrocoagulation and electrodialysis are effective, but their high run-cost limits their further application.<sup>12</sup>

Constructed rapid infiltration systems (CRIS), which were developed based on the conventional rapid infiltration system (RIS), is a new type of wastewater treatment system and have been widely applied in practical engineering, which can remove pollutants effectively in municipal sewage and resist impact load.<sup>13</sup> Phosphorus removal mechanisms of CRIS mainly include substrate adsorption and stabilization by microbial growth. The core of CRIS is to choose well-penetrative natural river sand, ceramicsite, gangue as infiltration media to replace the natural soil layer.<sup>14</sup> Zeolites are hydrated crystalline aluminum–silicate materials with a framework structure, where

School of Civil Engineering and Architecture, Wuhan University of Technology, 122, Luoshui Road, Hongshan District, Wuhan, China, 430070. E-mail: ZXLCL@126.com; Tel: +86 13808670309

† Electronic supplementary information (ESI) available. See DOI: 10.1039/c9ra04826j



their micro- and mesopores are occupied by water and typically alkaline cations.<sup>15</sup> Actually, original zeolites have been used as cationic exchange materials for the remediation of contaminants due to their excellent properties as adsorbents.<sup>11</sup> During the last decade, alternative and novel modifications have rapidly become important because they endow zeolites with potential to behave as anionic exchangers. The hybrid system consisting of a coarse zeolite trickling filter conducted by Luo *et al.* displayed excellent COD<sub>Cr</sub>, TP and ammonium removal performance.<sup>11</sup>

However, some problems that lower the phosphorus removal rates still exist. Therefore, selecting suitable modification methods for zeolites is essential for the CRIS design when considering the longevity of CRIS. In particular, adsorption and precipitation reach saturation easily on the adsorption sites during pollutant treatment, thus decreasing the treatment efficiency.<sup>16</sup> Hence, it has been a research hotspot for many researchers in the field of wastewater treatment to find some novel methods to improve phosphorus treatment performance of CRIS with zeolite substrates.

Layered double hydroxides (LDHs) have a structure that is analogous to naturally occurring hydrotalcite,<sup>17</sup> consisting of cationic brucite layers and exchangeable interlayer anions. Most LDHs can be nominally expressed as the chemical formula  $[M_{1-x}^{2+}M_x^{3+}(\text{OH})_2]^{x+}(A^{n-})_{x/n} \cdot m\text{H}_2\text{O}$ , where  $M^{2+}$  represents a divalent metal cation,  $M^{3+}$  represents a trivalent metal cation and  $A^{n-}$  represents an anion.<sup>18</sup> In general, the values of  $x$  range between 0.13 and 0.33. Due to their positively charged brucite-like sheets and relatively weak interlayer bonding, LDHs typically exhibit excellent affinity to various anions such as non-metal oxyanions, anionic metal complexes, organic anions and anionic polymers.<sup>19</sup> Because of their excellent adsorption ability to anions, LDHs have been suggested to be potential adsorbents to remove phosphorus from contaminated water.<sup>20</sup> However, the application of LDHs powders as adsorbents or catalysts still has some drawbacks, such as the aggregation of particles and difficulty in their separation, regeneration and reusability.<sup>21</sup> Meanwhile, powdered LDHs aggravate the existing bottlenecks due to their small size, low specific density and subsequent solid/liquid separation process when applied in CRIS. In addition, the high cost of pure LDHs should also be considered. Therefore, considering powered LDHs and common substrates comprehensively, we hope to adopt their advantages and avoid their disadvantages.

Additionally, there are few studies about the microbial properties of CRIS focusing on the microbial community structure and spatial distribution.<sup>22</sup> To explore the deep mechanisms in microbial factor for phosphorus removal, high-throughput sequencing technologies were utilized to research the structure of complicated bacterial assemblies attached on substrate particles in water and wastewater treatment bioreactors.<sup>23</sup>

As a continuation of our previous work,<sup>24–28</sup> four types of different Zn-LDHs (Zn : Fe = 2 : 1/3 : 1 or Zn : Al = 2 : 1/3 : 1) were synthesized and *in situ* coated on the original zeolites. Subsequently, lab-scale simulated CRIS were assembled to investigate the phosphorus removal performance and

mechanism of the Zn-LDHs-modified zeolites. The aims of this study include: (1) to evaluate the phosphorus removal performance of different Zn-LDHs-modified zeolites as substrates of CRIS during purification experiments; (2) to determine the optimal combination of metal compounds or molar (M) ratio and discuss the adsorption mechanism of phosphorus removal through isothermal adsorption-desorption and adsorption kinetic experiments; and (3) to analyze bacterial communities for the determination of their relationship with system performance and investigate the bacterial abundance and dominant bacterial population through high-throughput sequencing in the lab-scale simulated CRIS.

## Materials and methods

### Design and operation of the simulated CRIS

All purification experiments were operated in a lab-scale simulated CRIS. The simulated CRIS was assembled indoors with 10 experimental columns (0.4 m in length and 0.08 m in diameter) made of polyvinyl chloride (PVC) pipes, which were defined as 1A, 2A, 3A, 4A, and 5A (Group A), and 1B, 2B, 3B, 4B, and 5B (Group B, whose microbial growth was inhibited by adding chloroform). Each column was filled with the Zn-LDHs-modified or original zeolites, whose filling height was approximately 0.35 m. The experimental column numbers and types of modified zeolites are presented in Table 1.

Derived from a septic tank in the Wuhan University of Technology, the influent flowed into the columns from the top and out from the bottom. The hydraulic retention time (HRT) was 24 h under intermittent conditions and the hydraulic loading was 120 L (m<sup>2</sup> d)<sup>−1</sup>. After the reactor ran stably, eight consecutive experiments (labeled as 1, 2, 3, 4, 5, 6, 7, and 8) were conducted at time order. The water quality of influent of each experiment was varied to some extent. The content of phosphorus in the raw influent ranged from 2.537 to 6.616 mg L<sup>−1</sup> (total phosphorus, TP), from 2.537 to 6.028 mg L<sup>−1</sup> (total dissolved phosphorus, TDP), from 2.352 to 5.464 mg L<sup>−1</sup> (soluble reactive phosphorus, SRP). Also, the standard deviation of TP, TDP and SRP was 1.314, 1.433 and 1.291 mg L<sup>−1</sup>, respectively.

### Preparation of the LDHs-modified zeolites

The original zeolites were purchased in Zhengzhou city, Henan province, China. The diameter of the original zeolites was 2.0–4.0 mm, their true and bulk densities were 1.93 g cm<sup>−3</sup> and 1.32 g cm<sup>−3</sup>, respectively and their average voidage was 31.61%.

Four types of LDHs-modified zeolites were prepared from their respective metallic chloride salts (AR), including Zn-Fe (Zn : Fe = 2 : 1/3 : 1) and Zn-Al (Zn : Al = 2 : 1/3 : 1). The ZnFe-LDHs-modified (Zn : Fe = 2 : 1) zeolites were set as an example to describe the specific Zn-LDHs-modified method. *Via* the co-precipitation method, the above LDHs coatings were synthesized under alkaline conditions by simultaneously adding aqueous solutions of ZnCl<sub>2</sub> and FeCl<sub>3</sub> (Zn<sup>2+</sup> : Fe<sup>3+</sup> molar ratio of 2 : 1) to a 2 L beaker containing the original zeolites, and then heated to maintain a temperature of 80 °C. Meanwhile, an appropriate volume of 10 wt% NaOH solution was added to



Table 1 Experimental column numbers and corresponding modification ways

Column number	1A	2A	3A	4A	5A
Modification	ZnFe-LDHs (2 : 1)	ZnAl-LDHs (2 : 1)	ZnFe-LDHs (3 : 1)	ZnAl-LDHs (3 : 1)	Original
Column number	1B	2B	3B	4B	5B
Modification	ZnFe-LDHs (2 : 1)	ZnAl-LDHs (2 : 1)	ZnFe-LDHs (3 : 1)	ZnAl-LDHs (3 : 1)	Original

maintain the pH at approximately 11 under continuous stirring for 4 h. After complete precipitation, the mixed compounds were centrifuged at a speed of 1000–1500 rpm for 10 min and washed thoroughly with de-ionized water until the pH of the final effluent solution was neutral. Finally, the washed samples were oven-dried for 16 h to obtain the ZnFe-LDHs-modified (2 : 1) zeolites. Other Zn-LDHs-modified zeolites were synthesized *via* an analogous method. Each type of Zn-LDHs-modified and original zeolite was filled into the corresponding experimental columns (Table 1).

### Characterization methods

Morphological features were examined *via* scanning electron microscopy (SEM, JSM-5610, Japan) with energy dispersive X-ray (EDX, Oxford X-MAX). Powder X-ray diffraction (XRD) measurements were performed on a D8 ADVANCE and DAVINCI Design by using Cu K $\alpha$  radiation ( $\lambda = 0.154$  nm) at 45 kV and 40 mA with a scanning rate of  $5^\circ \text{ min}^{-1}$  in the  $2\theta$  range of  $5^\circ$  to  $85^\circ$ . Brunauer–Emmett–Teller (BET) surface areas of the zeolites were analyzed by N<sub>2</sub> adsorption on a BELSORP-Max\_MicrotracBEL (Japan). Besides, after the purification experiments, all the zeolites were retrieved and characterized by EDX, revealing the mechanisms of phosphorus removal on the other side.

### Water quality monitoring methods

The effluent was collected from the bottom of the simulated experiment columns for wastewater treatment analysis. Laboratory analyses were performed on the water sample for total TP, TDP and SRP. All the above parameters were determined based on standard methods<sup>29</sup> using an ultraviolet spectrophotometer (UV-1100 spectrophotometer, MAPADA Instrument Manufacturing Co., Ltd.). The concentration of Cl<sup>−</sup> was detected by ion chromatograph (Dionex ICS-900, Thermo Fisher Scientific, USA).

### Adsorption isothermal experiments

The original and Zn-LDHs-modified zeolites were utilized in adsorption isothermal experiments. For the adsorption of phosphate, stock solutions were prepared from KH<sub>2</sub>PO<sub>4</sub> (guarantee reagent, GR). The adsorption experiments were conducted in a series of 250 mL conical flasks using 100 mL KH<sub>2</sub>PO<sub>4</sub> solution at the initial phosphate concentration from 0 to 64 mg L<sup>−1</sup> with the substrate dosages of 10 g. The mixtures were shaken at the speed of 120 rpm in thermostatic water bath shaker (SHZ-82, Changzhou Guohua Instrument Manufacturing Co., Ltd.) at  $25 \pm 1^\circ \text{C}$  for 24 hours. The substrates were separated from the mixture by filtration after shaking at once. The filtrates were measured for the residual phosphate concentration in solution

using the standard methods.<sup>29</sup> All experiments were carried out in duplicate.

The phosphate adsorption capacities of the original and LDHs-modified zeolite substrates were determined from the following eqn (1):

$$q_e = \frac{(C_0 - C_e)}{m} \quad (1)$$

where  $C_0$  and  $C_e$  are the initial and equilibrium concentration of phosphate in solution (mg L<sup>−1</sup>), respectively,  $q_e$  is the equilibrium adsorption capacity (mg kg<sup>−1</sup>),  $m$  is the dry adsorbent weight (kg), and the  $V$  is the suspension volume (L).

Within the above optimized conditions, the adsorption isotherms of the original and LDHs-modified zeolite substrates were studied at  $25 \pm 1^\circ \text{C}$ . The data was used to plot the linearly transformed Langmuir equation (eqn (2)) and Freundlich equation (eqn (3)).

$$\frac{C_e}{q_e} = \frac{1}{K_1 q_m} + \frac{C_e}{q_m} \quad (2)$$

$$\lg q_e = \lg K_f + \frac{1}{n} \lg C_e \quad (3)$$

where  $C_e$  is the equilibrium concentration of phosphate in solution (mg L<sup>−1</sup>),  $q_e$  is the amount of phosphate adsorbed at equilibrium (mg kg<sup>−1</sup>),  $q_m$  is the theoretical maximum sorption capacity (mg kg<sup>−1</sup>),  $K_1$  is the Langmuir adsorption equilibrium constant, which is related to the energy of adsorption,  $K_f$  is Freundlich adsorption equilibrium constant, and  $n$  is a constant, which represents the Freundlich isotherm curvature.

### Desorption experiments

Based on previous research,<sup>26</sup> the desorption reagents were finally determined to be 5 M NaCl and 0.1 M NaOH after a series of preliminary desorption experiments. The adsorbent was separated from the mixture by filtration after the adsorption experiments and washed in deionized water several times to remove the unadsorbed phosphate. The washed adsorbent was mixed with 50 mL 5 M NaCl and 50 mL 0.1 M NaOH at the speed of 120 rpm in a thermostatic water bath shaker at  $25 \pm 1^\circ \text{C}$  for 24 h. The desorbed phosphate was analyzed by standard methods.<sup>26</sup>

### Ion exchange detection experiments

The as-prepared Zn-LDHs-modified or original zeolites with a dose of 10 g after washing with deionized water were placed into 5 conical flasks, as the experimental group. The above process was duplicated and set as the control group. Then,



500 mL 4 mg L<sup>-1</sup> KH<sub>2</sub>PO<sub>4</sub> solution was added to the 5 conical flasks in the experimental group. Meanwhile, 100 mL deionized water was added to the remaining 5 conical flasks in the control group, which was for eliminating the influence of deionized water. Subsequently, the solid-liquid mixtures were shaken at a speed of 120 rpm in a thermostatic water bath shaker at 25 °C for 12 h. The concentrations of Cl<sup>-</sup> in the filtrates were measured by ion chromatograph (Dionex ICS-900, Thermo Fisher Scientific, USA) to estimate the ion exchange capacities. The concentrations of Cl<sup>-</sup> in filtrate were calculated using the following equation:

$$C_i = C_0 - C_e \quad (4)$$

where  $C_e$  (mg L<sup>-1</sup>) is the concentration of Cl<sup>-</sup> in the experimental group,  $C_0$  (mg L<sup>-1</sup>) is the concentration of Cl<sup>-</sup> in the control group, and  $C_i$  (mg L<sup>-1</sup>) is the concentration of Cl<sup>-</sup> by ion exchange.

### Adsorption kinetic experiments

The phosphate adsorption kinetic experiments were carried out by adding 10 g adsorbent (original or Zn-LDHs-modified zeolites substrates) to a 250 mL flask filled with 100 mL phosphate solution at the initial concentration of 4 mg-P L<sup>-1</sup>. The conical flasks were placed in thermostatic shaker at 25 ± 1 °C and shaken at 120 rpm. The subsequent detection procedures were similar to that for the phosphate isothermal adsorption experiments. All experiments were carried out in duplicate.

The amount of phosphate adsorbed on the adsorbents at time,  $t$ , was calculated using the following equation (eqn (5)):

$$q_t = \frac{(C_0 - C_t)V}{m} \quad (5)$$

where  $C_0$  (mg L<sup>-1</sup>) is the initial concentration of phosphate in solution, and  $C_t$  (mg L<sup>-1</sup>) is the concentration of phosphate at setting time  $t$  (h),  $q_t$  (mg kg<sup>-1</sup>) is the amount of phosphate adsorbed at time  $t$  (h),  $m$  (kg) is the dry weight of adsorbent, and  $V$  (L) is the suspension volume.

In order to illuminate the adsorption kinetics of phosphate on the original and Zn-LDHs-modified zeolites, the data from the adsorption kinetic experiments was fitted with the pseudo-first-order (eqn (6)) and pseudo-second-order (eqn (7)) equations:

$$\lg(q_e - q_t) = \lg q_e - \frac{K_1}{2.303} t \quad (6)$$

$$\frac{t}{q_t} = \frac{1}{K_2 q_e^2} + \frac{t}{q_e} \quad (7)$$

where  $q_e$  (mg kg<sup>-1</sup>) and  $q_t$  (mg kg<sup>-1</sup>) are the amount of phosphate adsorbed on the adsorbents at equilibrium and at time  $t$  (h), respectively.  $K_1$  (h<sup>-1</sup>) is the rate constant of the pseudo-first-order, which was calculated by plotting  $\lg(q_e - q_t)$  versus  $t$  from the adsorbent samples. Additionally, based on the experimental data of  $q_t$  (mg kg<sup>-1</sup>) and  $t$  (h), the equilibrium adsorption capacity,  $q_e$  (mg kg<sup>-1</sup>), and the pseudo-second-order model rate

constant ( $K_2$ ) was determined from the slope and intercept of the plot of  $t/q_t$  versus  $t$ , respectively.

The intra-particle diffusion model (eqn (8)) based on the theory proposed by Weber and Morris<sup>30</sup> was applied to elucidate the diffusion mechanism. According to this model:

$$q_t = K_{di} \sqrt{t} + c_i \quad (8)$$

where  $K_{di}$  is the intra-particle diffusion rate constant (mg (g h<sup>1/2</sup>)<sup>-1</sup>). If intra-particle diffusion is rate-limited, then the plot of adsorbate uptake,  $q_t$ , versus the square root of time ( $t^{1/2}$ ) will result in a linear relationship.

### Microbial high-throughput sequencing in simulated CRIS

After the purification experiments, the samples of original and Zn-LDHs-modified zeolites were retrieved from experimental columns. Then the fractions of substrates were entrusted to conduct microbial high-throughput sequencing in Personal Biotechnology Co., Ltd, Shanghai, China. The whole processes included DNA extraction, PCR amplification and high-throughput sequencing and was performed in an Illumina MiSeq platform.

### Statistical analysis

The statistical analyses were mainly performed using the Origin (v8.0) and Statistical Product and Service Solutions (SPSS 19.0) software, including ANOVA. Post hoc multiple comparisons (Bonferroni Test) were also performed to test for statistically significant differences in the LDHs-modified zeolites. A statistically significant difference was defined as  $p < 0.05$  and the  $p$  value also denoted the significant (two-tailed) value in the test. The XRD data was analyzed using the MDI Jade (v6.0) software and relevant images were obtained using the Origin (v8.0) software.

## Results

### Characterization of physicochemical properties

SEM was conducted to observe the surface morphological structure of all the Zn-LDHs-modified and original zeolites before and after the purification experiments. Firstly, the SEM images of ZnAl-LDHs-modified (3 : 1) (a), ZnFe-LDHs-modified (3 : 1) (b) and original (c) zeolites were chosen as representatives, as shown in Fig. 1. The SEM images shown in Fig. 1a–c indicated that there were some layered sundries like scales on the surface of the zeolites. However, Fig. 1a and b further reveal some relatively obvious hexagon overlapping crystals like stacked layers, which are typical for LDHs. The special morphology features shown in Fig. 1a and b are similar to that observed in Wang's study.<sup>31</sup> The well-marked labels in Fig. 1a and b highlight that special surface morphological structure was responsible for the LDH materials. Besides, compared with the SEM images (Fig. 1a–c) before the purification experiments, the hexagon overlapping crystals disappeared, which may be covered by the phosphorous adsorbed on them after the purification experiments, as shown in Fig. 1d–f, respectively.





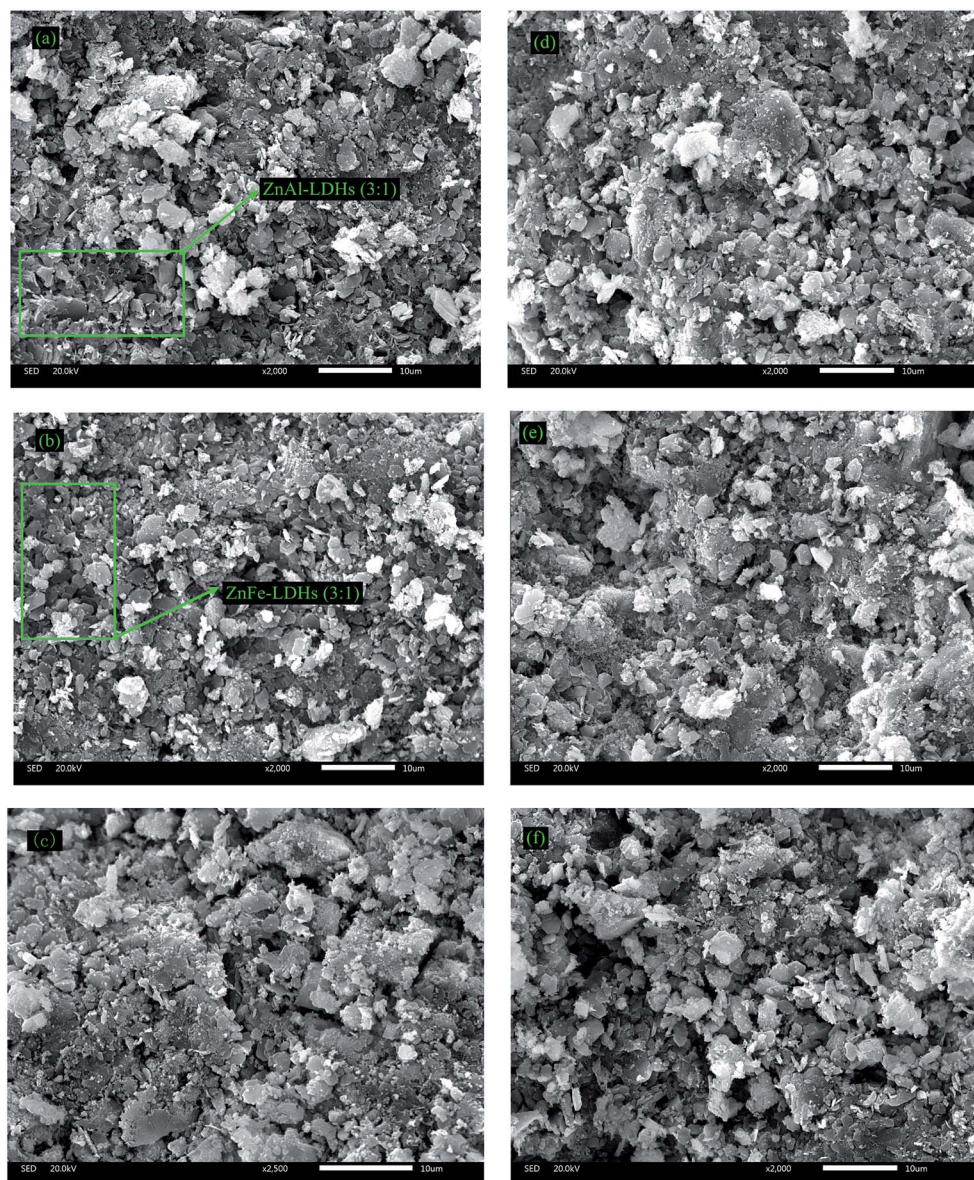


Fig. 1 SEM images of ZnAl-LDHs-modified (3 : 1), ZnFe-LDHs-modified (3 : 1) and original zeolites substrates before (a–c) and after (d–f) the purification experiments (resolution ratio: 10  $\mu\text{m}$ ).

Next, to better describe the chemical components and element percentage (%) in the Zn-LDHs-modified and original zeolites, EDX was conducted to determine the particular chemical elements and their relative contents. The EDX images and statistics of the Zn-LDHs-modified and original zeolites are presented in Fig. S1 and Table S1,<sup>†</sup> respectively. By comparing the EDX images of all the Zn-LDHs-modified and original zeolites in Fig. S1,<sup>†</sup> it can be found that the Cl element on appeared in all the Zn-LDHs-modified zeolites. Since the Zn-LDHs were synthesized using different types of trivalent metal chloride and then coated on the zeolites, the as-prepared Zn-LDHs-modified zeolites were also termed Zn-LDHs-Cl-modified zeolites actually. Therefore, the successful coating of the as-prepared Zn-LDHs and feasibility of the LDH modification strategy could be effectively verified. As presented in Table S1,<sup>†</sup> the Zn contents of both the Zn-LDHs (2 : 1) modified

and original zeolites were lower than that of Zn-LDHs (3 : 1) modified zeolites, which is a feature of synthetic Zn-LDHs with different  $\text{M}^{2+}/\text{M}^{3+}$  ratios.

Furthermore, we also conducted XRD material testing (Fig. S2<sup>†</sup>). Initially, the pure Zn-LDHs and corresponding Zn-LDHs-modified zeolites were prepared simultaneously to verify the successful synthesis of Zn-LDHs on the surface of the modified zeolites. Subsequently, the as-prepared pure Zn-LDHs were defined as X1, X2, X3 and X4 (ZnAl-LDHs (2 : 1), ZnAl-LDHs (3 : 1), ZnFe-LDHs (2 : 1) and ZnFe-LDHs (3 : 1), respectively). Additionally, through low-speed stirring, ultrasonic cleaning and vacuum infiltration after adding a moderate amount of distilled water to the four types of LDHs-modified zeolites, the materials covering the Zn-LDHs-modified zeolites were acquired and dried, named X5, X6, X7 and X8 with same sequence of naming as pure Zn-LDHs, respectively. The original



zeolites were ground into a powdered state and named X9. By comparing the XRD images of X1, X5 and X9 (X2, X6 and X9, or X3, X7 and X9, or X4, X8 and X9), the successful coating of Zn-LDHs was also demonstrated.

As illustrated in Fig. S2a,† a series of peaks appeared as sharp and intense symmetric lines at low  $2\theta$  values and clear reflections at high  $2\theta$  values for X1 and X5, indicating the characteristic basal reflection of hydrotalcite-like ZnAl-LDHs materials.<sup>32</sup> Strong peaks corresponding to the (003) and (006) faces were observed and the angle of the peak of (003) indicated a larger distance between the inter-layer.<sup>33</sup> Meanwhile, compared with the XRD pattern of X9, there was nearly no typical peak at the (003) or (006) faces. This indicates that the ZnAl-LDHs could be synthesized and coated on the surface of zeolites from another side. The situations shown in Fig. S2b† are similar to that in Fig. S2a.† The (003) and (006) peaks appeared for X2 and X6, which were different from X9 conspicuously. Besides, as shown in Fig. S2c,† the XRD peaks for the ZnFe-LDHs exhibited high consistency with the characteristic peaks of hydrotalcite-like LDH with hexagonal lattice (X3 and X7). The detected diffraction peaks were consistent with the crystallographic planes of (006), (009), (015) and (113), which can be indexed to typical LDH materials.<sup>34</sup> The higher reflection intensity illustrates the higher degree of crystallization for the prepared LDHs. Finally, the specific conditions shown in Fig. S2d† are similar to that in Fig. S2c.† The XRD pattern of X9 did not exhibit the (006), (009), (015) and (113) peaks. According to the above XRD description all the samples, the synthesis and coating were successfully demonstrated, which indicates that the co-precipitation method utilized in our study is convincing and feasible.

## Purification experiments

In purification experiments, the removal rates of TP, TDP and SRP and average removal rates by the Zn-LDHs-modified and original zeolites in Group A and B during the purification period are shown in Fig. 2.

According to Fig. 2, all the Zn-LDHs-modified zeolites performed better than the original zeolites whether in Group A or B, and the performance of the Zn-LDHs-modified zeolites maintained a higher level in removing phosphorus. For TP removal, the average rates for the Zn-LDHs-modified zeolites were over 80%, except for the ZnAl-LDHs-modified (2 : 1) zeolites. According to Fig. 2d, 3A (85.72%) and 4A (80.76%) performed better than 1A (80.63%), 2A (57.77%) and 5A (18.04%) for TP removal. Compared with that of 5A (18.04%), the increment in the TP average removal rates of 1A–4A was 62.59%, 39.73%, 67.68% and 62.72%, respectively. This indicates that the TP average removal rates could be improved by Zn-LDHs coating strategy significantly, especially the ZnFe-LDHs (3 : 1) coating. Comparing the Zn-LDHs-modified (2 : 1) and (3 : 1) zeolites, the Zn-LDHs-modified (3 : 1) zeolites performed better than the Zn-LDHs-modified (2 : 1) zeolites whether  $M^{3+}$  was  $Fe^{3+}$  or  $Al^{3+}$ .

Additionally, 1A/3A (85.84% and 88.81%) still performed better than 2A/4A/5A (60.22%, 84.90% and 21.31%) for TDP

removal (Fig. 2d), respectively. Overall, the increment in the TDP removal rate of 1A–4A was 64.53%, 38.91%, 67.50% and 63.59% in comparison with that of the original zeolites, respectively. This indicates that the TDP removal rate can be improved by the Zn-LDHs coating method, especially using ZnFe-LDHs (3 : 1), which is in accordance with purification experimental results for the TP removal rates. Meanwhile, whether  $M^{2+} : M^{3+}$  was 2 : 1 or 3 : 1, the ZnFe-LDHs-modified zeolites always performed better than the ZnAl-LDHs-modified zeolites for TDP removal.

1A/3A (85.85% and 87.55%) performed better than 2A/4A/5A (54.60%, 79.00% and 22.04%) for SRP removal (Fig. 2d). The increment in the SRP removal rate of the 1A–4A was 63.81%, 32.55%, 65.51% and 56.96%, respectively, compared with that of the original zeolites, indicating that the SRP removal rate can be increased using the Zn-LDHs coating method, especially ZnFe-LDHs (3 : 1). Similarly to the experimental results of TP and TDP removal,  $Fe^{3+}$  was more beneficial than  $Al^{3+}$  for SRP removal.

According to the results of one-way ANOVA of TP, TDP and SRP removal, a statistically significant difference was observed between the Zn-LDHs-modified and original zeolites. This proved that all the removal rates of TP, TDP and SRP could be significantly improved *via* the Zn-LDHs coating method.

Comparing Group A and Group B in Fig. S3,† it can be found that Group A performed better than Group B in removing TP, TDP and SRP. The microbial effects of the purification experiments were highlighted by comparing Group A with Group B. The microbial action by the Zn-LDHs-modified and original zeolites was obtained by subtracting the removal rates of 1A–5A from that of 1B–5B, respectively. According to Fig. S3,† compared with that of the original zeolites, the microbial effects were boosted by the Zn-LDHs coating method, especially using the ZnAl-LDHs (3 : 1) coating.

## Adsorption experiments

**Isothermal adsorption experiments.** Considering the higher removal performance of the Zn-LDHs-modified zeolites in the purification experiments, batch adsorption experiments were performed to investigate the adsorption capacities of the Zn-LDHs-modified and original zeolites. The adsorption isotherms are the mathematical models and the adsorption capacity is illustrated at different aqueous equilibrium concentrations.<sup>35</sup> The Langmuir and Freundlich isotherms were adopted to describe the relationship between the amount of phosphate adsorbed and its equilibrium concentration in solution. The corresponding constants and regression coefficients of the Langmuir and Freundlich equations are presented in Table 2. The Langmuir isotherm gave a slightly better fitting to the adsorption isotherms of 3A, 4A and 5A, especially 5A according to the  $R^2$  values from Table 2. This suggests that the adsorption of phosphate is attributed to monolayer adsorption on the outer surface of the adsorbent. However, the results of 1A and 2A indicate that the Freundlich equation fitted better than the Langmuir equation, manifesting the adsorption of phosphate is attributed to multilayer adsorption on the outer surface of the adsorbent.<sup>4</sup>





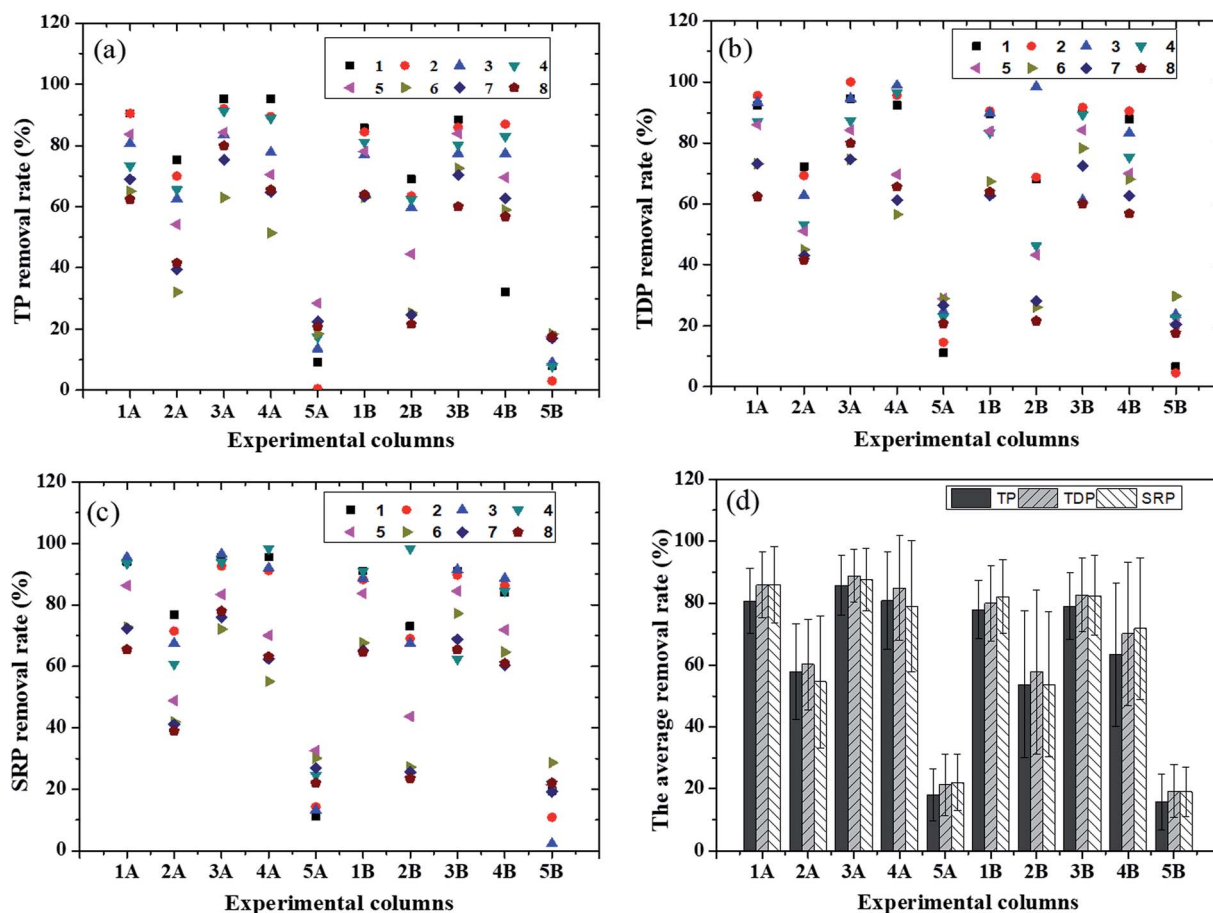


Fig. 2 Removal rates of total phosphorus (TP) (a), total dissolved phosphorus (TDP) (b), soluble reactive phosphorus (SRP) (c) and average removal rates (d).

Table 2 The fitting parameters of the Freundlich and Langmuir models for the Zn-LDHs-modified and original zeolites

Adsorbent	Langmuir isothermal model			Freundlich isothermal model		
	$K_L$	$q_m$	$R^2$	$K_f$	$n$	$R^2$
1A	0.3295	344.83	0.9439	76.6539	2.3861	0.9535
2A	0.3622	217.39	0.9703	56.2553	2.7693	0.9790
3A	0.5349	434.78	0.9747	101.9008	1.9697	0.9609
4A	0.4203	344.83	0.9746	77.4707	2.1566	0.9726
5A	0.4397	196.08	0.9975	43.2588	2.0404	0.9255

The constants of  $K_f$  and  $n$  in the Freundlich equation are associated with the adsorption capacity and adsorption intensity, respectively. The constant  $n$  is a measure of the exchange intensity of the surface heterogeneity, and a higher  $K_f$  value represents a larger adsorption capacity. From Table 2, The  $K_f$  values of 1A–4A were larger than that of 5A, indicating that the adsorption capacity could be improved *via* the Zn-LDHs coating method. Additionally, the maximum theoretic adsorption capacities ( $q_m$ ) of 1A–5A are shown in Table 2, which follow the order: 3A > 4A = 1A > 2A > 5A.

**Desorption studies.** After the adsorption experiments, desorption experiments were performed to study the desorption properties of all the zeolites. Upon adding the isometric desorption reagent solution after reaching adsorption equilibrium at an initial phosphate concentration of  $8 \text{ mg L}^{-1}$  on the adsorbents, the desorption rates of 1A–5A were calculated to be 37.34% (1A), 40.81% (2A), 39.24% (3A), 38.67% (4A) and 30.38% (5A) (2A > 3A > 4A > 1A > 5A). It was observed that the desorption rates of all the Zn-LDHs-modified zeolites were higher than that of the original zeolites. The relatively higher desorption rates of the Zn-LDHs-modified zeolites indicates that the Zn-LDHs coating method is more efficient in regeneration for subsequent application as an adsorbent. This is relatively significant and economical when applied in the practical CRIS.

**Adsorption kinetic experiments.** Besides, this study aimed at uncovering the deeper adsorption mechanisms. The adsorption kinetics is important for adsorption studies because it can predict the rate of adsorbate uptake on adsorbents, control the equilibrium time and provide valuable data for understanding the mechanism of the adsorption reaction.<sup>36</sup> Fig. S4† presents the fitting results of the adsorption kinetic experimental data for the pseudo-first-order (Fig. S4a†) and pseudo-second-order (Fig. S4b†) models.



**Table 3** Pseudo-first order and pseudo-second order adsorption kinetic constants of Zn-LDHs-modified and original zeolites (the initial concentration = 4 mg L<sup>-1</sup>)

Adsorbent	$q_e$	Pseudo-first-order			Pseudo-second-order		
		$q_{e,cal}$	$K_1$	$R^2$	$q_{e,cal}$	$K_2$	$R^2$
1A	28.35	19.53	0.200	0.971	27.54	0.027	0.977
2A	33.40	14.17	0.141	0.822	30.49	0.052	0.984
3A	26.40	19.37	0.263	0.950	29.41	0.020	0.978
4A	25.05	19.96	0.232	0.968	27.93	0.016	0.971
5A	16.12	16.42	0.120	0.978	17.09	0.066	0.972

According to the values of the correlation coefficient ( $R^2$ ) (Table 3), the pseudo-second order model can describe the adsorption kinetics data for phosphate better than the pseudo-first-order model for 1A–4A. However, the fitting result of 5A, was described better by the pseudo-first order model, contrary to that of 1A–4A. Moreover, the calculated equilibrium adsorption capacities ( $q_{e,cal}$ ) (mg kg<sup>-1</sup>) were much closer to the experimental values  $q_e$  (mg kg<sup>-1</sup>), implying the overall rate of the adsorption process was controlled by chemisorption.<sup>37</sup>

Additionally, the intra-particle diffusion equation was utilized to further explore the diffusion mechanisms. From the corresponding equation parameters given in Table S2,†  $C_i$  represents the thickness of the boundary layer. If the value of  $C$  is zero, the rates of adsorption are controlled by intra-particle diffusion for the entire adsorption process. Generally, the plots of  $q_t$  against  $t^{1/2}$  showed more than one linear portion, implying that more than one process affected the adsorption. According to the fitting results given in Table S2,† the adsorption process included three stages, which are external surface adsorption stage, gradual adsorption stage and desorption stage.

It should be highlighted that the values of  $K_{d2}$  for the Zn-LDHs-modified zeolites were larger than that of the original zeolites, indicating that the gradual adsorption of the Zn-LDHs-modified zeolites was faster to reach adsorption equilibrium

than that of original zeolites. The reason for this may be that Zn-LDHs-modified zeolites had a larger surface area and pore volume for solution adsorption instantaneously. Therefore, the adsorption process could be accelerated by the Zn-LDHs coated on the surface of the original zeolites, which is beneficial for reducing the time costs by improving the adsorption efficiency in practical CRIS.

**Microbial high-throughput sequencing.** Remarkably, to further explore the microbial mechanisms of phosphorus removal, the microbial diversity and abundance were tested by high-throughput sequencing to illustrate the phylogenetic difference in the compositions of the bacterial structures of lab-scale simulated CRIS. There were 164 920 high-quality sequences in total for five samples. The maximum and minimum OTUs were shown on sample 5A and sample 1A, respectively, as presented in Table S3.†

Microbial diversity and abundance indexes were calculated using the Mothur software at 97% sequence identity. The Chao 1 index and Abundance-based Coverage Estimator (ACE) index were utilized to describe the microbial community abundance, where a higher value of Chao 1 and ACE index represents a higher abundance. Additionally, the Shannon-Wiener and Simpson are common indexes to assess microbial community diversity, where a higher value of Shannon-Wiener and Simpson index represent higher diversity. According to the values of the Chao 1 index (Table S3†), the five samples followed the order of 5A > 4A = 3A > 2A > 1A. According to the values of the ACE index, the five samples followed the order of 5A > 4A > 3A > 2A > 1A. Moreover, according to the values of the Shannon-Wiener index, the value of sample 1A was the lowest, and values of samples 1A–4A fluctuated slightly, which were lower than that of sample 5A. According to the values of the Simpson index, the values also varied a bit among 1A–5A, representing the order of 4A > 2A > 3A > 1A > 5A.

From Fig. 3a, there were high diversities for the bacterial community structure of the 5 samples (1A–5A) at the phylum level. Over 20 bacterial phyla were identified in the corresponding substrate samples derived from the experimental columns. The dominant bacteria reads in all the samples were

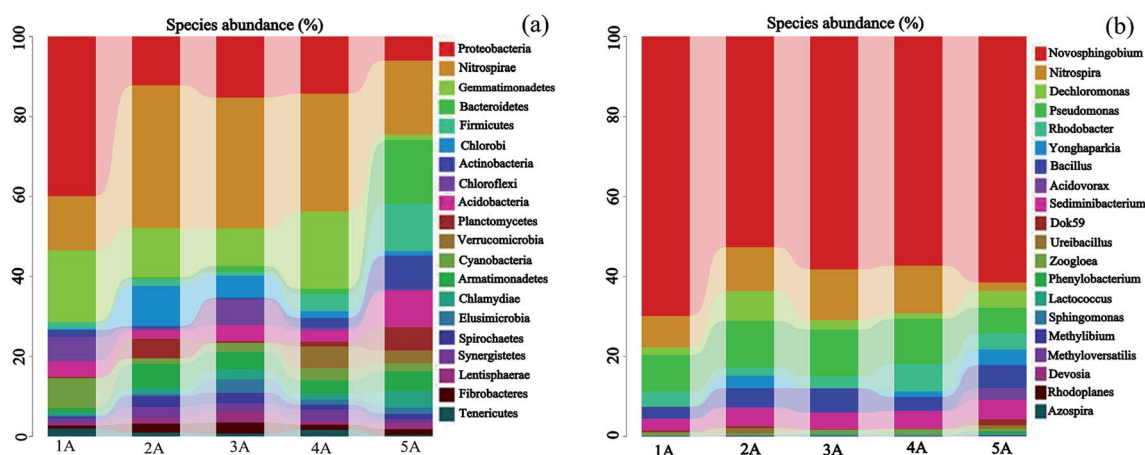


**Fig. 3** Bacterial community structure and distribution of the samples 1A–5A at the phyla (a) and genus (b) levels.





affiliated with two phyla, *Proteobacteria* (52.0–69.4%) and *Bacteroidetes* (6.4–11.6%), which can be of great significance for pollutant removal, including nitrogen or phosphorus removal.<sup>38</sup> The reads belonging to *Nitrospirae*, *Gemmatimonadetes*, *Firmicutes*, *Actinobacteria*, *Acidobacteria*, *Cyanobacteria*, *Chlorobi*, and *Chloroflexi* were found to be the minor groups. The microbial community composition was not totally in accordance with previous studies<sup>39</sup> because of the different inflow, which can provide different chemical and biological environments for microbial growth.

Among the five samples (1A–5A), the relative abundance of *Proteobacteria* for sample 1A (69.4%) was higher than that for samples 2A–5A (52.0%, 57.6%, 56.7%, and 60.2%), respectively. The relative abundance of *Bacteroidetes* for samples 1A–4A (9.2%, 11.6%, 11.6%, and 11.2%) was higher than that of sample 5A (6.4%), respectively. The *Proteobacteria*, including many bacterial genera for organic and inorganic metabolism, was widely distributed.<sup>40,41</sup> Meanwhile, many researchers have indicated that most bacteria affiliated to *Proteobacteria* play an important role in denitrification, biological phosphorus removal and organic matter degradation.<sup>42</sup> Additionally, Kragelund *et al.*<sup>43</sup> found that *Chloroflexi* have better bacterial phosphorus removal ability. In Fig. 3a, the relative abundance of *Chloroflexi* in sample 5A was the highest. However, the pollutant including phosphorus removal depends on the bacterial combined action, not a single bacterial action.

Besides, there were over 17 types of bacterial genera in the corresponding experimental columns, as shown in the Fig. 3b. The dominant genera were *Novosphingobium* (0.7–22.9%), *Nitrospira* (2.0–12.5%), *Dechloromonas* (0.1–0.3%) and *Pseudomonas* (0.1–1.8%). *Dechloromonas* and *Pseudomonas* play important roles in the transformation and cycle of phosphorus.<sup>44</sup> Obviously, the *Dechloromonas* and *Pseudomonas* abundances of sample 1A–4A (10.4%, 4.0%, 4.2% and 8.2%, respectively) were higher than that of sample 5A (2.0%), illustrating that relative abundance connected with phosphorus removal at the genus level increased owing to the Zn-LDHs coating method.

## Discussion

### Effects of adsorption on phosphorus removal

According to the results from the isothermal adsorption, the Zn-LDHs-modified zeolites performed better than the original zeolites in absorbing phosphate, which is attributed to their higher surface site area micro- and macro-porosity with abundant adsorption sites and macroporous networks with accessible diffusion pathways for adsorption reagents.<sup>45</sup> The unique three-dimensional frameworks with porosity on multiple length scales of Zn-LDHs coating are crucial for adsorption application in wastewater treatment. The results of isothermal adsorption experiments agree well with the results from the purification experiments, especially ZnFe-LDHs-modified (3 : 1) zeolites reaching 434.78 mg kg<sup>-1</sup>, which was the best performance among the Zn-LDHs-modified and original zeolites in our CRIS. The adsorption capacities of the ZnFe-LDHs-modified (3 : 1) zeolites reached 2.217 times that of the original zeolites. Additionally, the adsorption capacities of the Zn-Fe-LDHs-modified

zeolites were higher than that of the ZnAl-LDHs-modified zeolites whether  $M^{2+}/M^{3+}$  was 2 : 1 or 3 : 1. The results are consistent with Yang's study,<sup>46</sup> which indicated that ZnFe-LDHs have a large surface area and layered structure.

Meanwhile, the experimental data from the adsorption kinetic tests were fitted with pseudo-first-order, pseudo-second-order equation and intra-particle diffusion equations. The pseudo-first-order and pseudo-second-order models describe the kinetics of the solid-solution based on mononuclear and binuclear adsorption, respectively, with respect to sorbent capacity. The intra-particle diffusion model was chosen to investigate whether an intra-particle diffusion was a rate limiting factor in the adsorption process. According to the fitting results of the Zn-LDHs-modified and original zeolites, it was observed that the pseudo-second-order model gave a better fit for phosphate adsorption on the Zn-LDHs-modified zeolites, suggesting that the adsorption in this case was in fact a chemisorption process owing to the LDHs coating method. These results are consistent with previous studies, which reported that phosphate adsorption on LDHs is described by the pseudo-second-order mechanism.<sup>47</sup> Physical adsorption includes molecular attractive forces between the adsorbate and adsorbent, and this process requires less activation energy and is reversible. In contrast, chemical adsorption produces a chemical bond between the adsorbate and adsorbent, and this process needs a higher activation energy and is irreversible. Consequently, the predominant adsorption type can be transferred from intrinsically weak physical adsorption into tighter chemical adsorption, which is in accordance with Zhang's study.<sup>27</sup>

As shown in Table S2,<sup>†</sup> the plot was not linear over the entire time range and showed more than one linear portion, suggesting a multi-step process. Each step was identified by a change in the slope of the linear line, which was used to fit the experimental data. Thus, three linear regions were identified. Initially, the first region is attributed to the diffusion of phosphate through the solution to the external surface of the LDHs. Next, the second region describes the gradual stage in which the intra-particle diffusion is the rate limiting step and reaches the final equilibrium stage. Finally, the third region is attributed to the desorption stage, where intra-diffusion starts to slow down due to the low phosphate concentration in solution.<sup>48</sup> Hence, both the results of the intra-diffusion equation fitting that the adsorption process reaching adsorption equilibrium efficiently accelerated and the results of desorption that the regeneration became relatively higher by coating Zn-LDHs indicate that the Zn-LDHs coating on zeolites has potential as an recyclable and relatively cost-effective strategy in practical CRIS.

### Effects of microbial action on phosphorus removal

Besides the discussion of the removal mechanisms in adsorption, according to the results of the purification experiments (Fig. S3<sup>†</sup>), the microbial actions for phosphorus removal by the Zn-LDHs-modified zeolites were greater than that of the original zeolites. In Zhou's study,<sup>35</sup> there were some smaller meso-pores reflecting the pores present with nano-sheets and larger meso-



pores correlated to the pores formed between stacked nano-sheets of pure Zn-LDHs adsorbent materials. Generally, a larger surface area can offer more attachment sites. Therefore, with the Zn-LDHs coated on the surface of the original zeolites, the specific surface area of the original zeolites increased significantly for microbial attachment from  $7.120 \text{ m}^2 \text{ g}^{-1}$  to  $10.630 \text{ m}^2 \text{ g}^{-1}$ , which can provide more room for microorganisms that are beneficial for removing phosphorus. Meanwhile, it was significant that the Zn-LDHs-modified (3 : 1) coating had a bigger impact on microbial action than the Zn-LDHs-modified (2 : 1) coating, as shown in Fig. S3,† indicating the addition of Zn element, which is one of the essential elements for microorganisms, facilitated microbial growth.<sup>49</sup> Therefore, the novel hierarchical Zn-LDHs coating could increase the content of Zn element and augment the microbial attachment sites by increasing the specific surface area, and then influencing the microbial growth and action, which played an important role in phosphorus removal in our simulated CRIS.

Considering the relevant OTUs counts with microbial diversity and abundance indexes comprehensively, the microbial diversity decreased due to the Zn-LDHs coating on the zeolites. Additionally, the Shannon-Wiener index is more sensitive to diversity and rare OTUs of microbial community, whereas the Simpson index is more sensitive to evenness and preponderant OTUs. Based on the above orders of the Simpson's indexes of the five samples ( $4A > 2A > 3A > 1A > 5A$ ), as presented in Table S3,† it can be rationally inferred that much more preponderant microorganisms existed in 1A–4A compared with 5A. In the purification experiments, the microbial action was calculated using the difference in the phosphorus removal rates between Group A and B. Therefore, it can be conjectured rationally that the preponderant microorganisms in 1A–4A may be relevant to phosphorus removal. The microbial action plays a vital role in phosphorus removal in simulated CRIS. In summary, with the coating of Zn-LDHs on the zeolites, the microbial action was enhanced significantly through both augmenting the favorable Zn element, which is reported to be beneficial for microbial growth, and providing more attachment sites owing to the increase in the specific surface area.

### Integrated mechanism analyses for phosphorus removal

Overall, the adsorption and microbial action are the two main parts that contributed to the higher phosphorus removal performances in the purification experiments. According to the results of the purification experiments, the phosphorus removal rates of the Zn-LDHs-modified zeolites, which were over 80%, were higher than that in previous reports, such as Qin *et al.*<sup>50</sup> who reported that the phosphorus removal rates of zeolites modified by ferric trichloride reached 47%, and were higher than that of the original zeolites in our simulated CRIS. Although it is slightly lower than the maximum TP removal rates of the two-stage hybrid system consisting of a trickling filter and a horizontal flow multi-soil-layering bioreactor reported by Zhang *et al.* (92.0%)<sup>10</sup> and two-stage system consisting of an iron-modified zeolite trickling filter and a multi-soil-layering (consisting of zeolite permeable layers and soil

mixture block layers) reported by Luo *et al.* (92.0–94.0%),<sup>11</sup> the CRIS has many advantages, is easy to operate, and is cost-efficient compared with the above hybrid systems. The main mechanisms for phosphorus removal were adsorption, physical interception, ion exchange, and microbial action (Fig. S5†).

The peculiar structures of the double-layer metal hydroxides of LDHs with a positive charge affect the surface properties of zeolites, and thus their capacity of chemisorption, physical interception and microbial action directly or indirectly. According to the SEM results (Fig. 1) after the purification experiment, the hexagon overlapping crystals like a stacked layer, which are typical for LDHs, on the surfaces of the Zn-LDHs-modified zeolites disappeared, which may be because they were covered by the adsorbed phosphorous after the purification experiments. This reflects indirectly that some phosphorus particles were removed from the wastewater through physical interception. The nature of LDHs is the direct driving force for the formation of porous arrays with a house of cards, resulting in abundant inter-particle porosity.<sup>51</sup> Since the Zn-LDHs were coated on the zeolites, the content of metallic oxide increased, which is beneficial for forming insoluble metallic phosphate by ligand-exchange reactions with phosphate group adsorbed on metal ions.<sup>28</sup> Therefore, more PP-like metallic phosphate could be attached on the surface of the Zn-LDHs-modified zeolites.

It is generally believed that LDHs have greater affinities for anions with a higher charge density. Due to their relatively large surface areas and high anion-exchange capacity, LDHs have been previously employed in various studies. For common inorganic anions, the LDHs selectivity decreased in the following order:  $\text{CO}_3^{2-} > \text{PO}_4^{3-} > \text{SO}_4^{2-} > \text{Cl}^- > \text{NO}_3^-$ .<sup>19</sup> For the as-prepared Zn-LDHs-Cl-modified zeolites, ion exchange could occur between  $\text{PO}_4^{3-}$  and  $\text{Cl}^-$  efficiently, which is beneficial for phosphorus removal by the Zn-LDHs-modified zeolites. According to the results shown in Fig. S6,† it can be found that ion exchange indeed occurred between  $\text{PO}_4^{3-}$  and  $\text{Cl}^-$ . Conspicuously, the ion exchange capacities of the Zn-LDHs-modified (3 : 1) zeolites were superior to that of the Zn-LDHs-modified (2 : 1) zeolites. Meanwhile, there was barely an ion exchange in the original zeolites. Thus, it can be concluded that the Zn-LDHs coating method is advantageous to remove phosphorus by ion exchange. The specific adsorption and ion exchange mechanisms are shown in Fig. S7.†

The ZnFe-LDHs-modified zeolites performed better than the ZnAl-LDHs-modified zeolites for TP, TDP and SRP removal, which is in accordance with Yuan's study that substrates rich in Fe elements can be potential materials in improving phosphorus removal efficiently.<sup>52</sup> On the one hand, from the results of the isothermal adsorption experiments (Table 2), the Zn-LDHs coating enhanced the chemical adsorption capacities of the original zeolites, and then influenced the phosphorus concentration in the experimental columns. Concentrations of pollutants including phosphorus trended from high to low along the water flow direction in the experiment columns, which are beneficial for the enrichment of different functional microorganisms in distribution to make the species converge.<sup>53</sup> Thereby, the microbial diversity and structures made



a difference, which resulted in phosphorus removal during the purification experiments. On the other hand, the Zn-LDHs coating method affected morphological structure (Fig. 1) and chemical compositions on the zeolites. Both the microbial attachment sites and relevant elements with microbial growth increased, and the microbial action for phosphorus removal was enhanced in the purification experiments. Subsequently, the microorganisms related to phosphorus removal in turn promoted the phosphorus removal performance in the purification experiments. Eventually, it can be rationally concluded that the Zn-LDHs coating on the original zeolites is advantageous for removing phosphorus in CRIS. Moreover, the Zn-LDHs modified zeolites are expected to be prevailing substrates in practical CRIS effectively and sustainably, which is coincident with the initial purpose of our study.

## Conclusions

In this study, novel Zn-LDHs-modified ( $M^{2+}/M^{3+} = 2 : 1/3 : 1$ ) zeolites were synthesized *via* co-precipitation under alkaline conditions and filled into experimental columns to establish lab-scale simulated CRIS. From the results of the purification experiments, the removal rates of phosphorus (TP, TDP and SRP) significantly improved by coating Zn-LDHs on the original zeolites, especially the ZnFe-LDHs-modified (3 : 1) zeolites. According to the results of the adsorption experiments, the theoretical maximum adsorption capacities of all the Zn-LDHs-modified zeolites were efficiently promoted, especially that of the ZnFe-LDHs-modified (3 : 1) zeolites, reaching 434.78 mg kg<sup>-1</sup>. Desorption studies indicated that the regeneration rates improved *via* the Zn-LDHs coating method. The adsorption type was depicted to be more stable and tighter chemical adsorption based on the better fitting results of the pseudo-second-order model of the Zn-LDHs-modified zeolites. Additionally, the results of the intra-particle diffusion indicated that the adsorption process was accelerated by the Zn-LDHs coating. Some microbial genera relevant to phosphorus removal, such as *Dechloromonas* and *Pseudomonas*, increased significantly on the Zn-LDHs-modified zeolites during the purification experiments.

## Conflicts of interest

There are no conflicts to declare.

## Acknowledgements

This work was funded by the National Natural Science Foundation of China (No. 31670541, 31270573, 31400435). The authors also thank Material Research and Testing Center, Wuhan University of Technology for their technical support of the characteristics of the original and modified substrates.

## References

- 1 Y. Seida and Y. Nakano, Removal of phosphate by layered double hydroxides containing iron, *Water Res.*, 2002, **36**, 1306–1312.
- 2 J. J. Yuan, W. Y. Dong, F. Y. Sun, K. Zhao and P. Li, Enhanced heavy metal removal by wetland vegetations and its significance for vegetation-activated sludge process configuration, *Desalin. Water Treat.*, 2016, **57**, 25153–25160.
- 3 S. C. Ayaz, Ö. Aktas, N. Findik and L. Akca, Phosphorus removal and effect of adsorbent type in a constructed wetland system, *Desalin. Water Treat.*, 2012, **37**, 152–159.
- 4 J. B. Zhou, S. L. Yang, J. G. Yu and Z. Shu, Novel hollow microspheres of hierarchical zinc-aluminum layered double hydroxides and their enhanced capacity for phosphate in water, *J. Hazard. Mater.*, 2011, **192**, 1114–1121.
- 5 K. Zhou, B. Wu, L. S. Su, X. F. Gao, X. L. Chai and X. H. Dai, Development of nano-CaO<sub>2</sub>-coated clinoptilolite for enhanced phosphorus adsorption and simultaneous removal of COD and nitrogen from sewage, *Chem. Eng. J.*, 2017, **328**, 35–43.
- 6 L. L. Zhang, Q. Y. Yue, K. L. Yang, P. Zhao and B. Y. Cao, Enhanced phosphorus and ciprofloxacin removal in a modified BAF system by configuring Fe-C micro electrolysis: investigation on pollutants removal and degradation mechanisms, *J. Hazard. Mater.*, 2018, **342**, 705–714.
- 7 S. H. Lee, R. Kumar and B. H. Jeon, Struvite precipitation under changing ionic conditions in synthetic wastewater: experiment and modeling, *J. Colloid Interface Sci.*, 2016, **474**, 93–102.
- 8 Q. Zhou, Y. Lin, X. Li, C. P. Yan, Z. F. Han, G. M. Zeng, L. Lu and S. Y. He, Effect of zinc ions on nutrient removal and growth of *Lemna aequinoctialis* from anaerobically digested swine wastewater, *Bioresour. Technol.*, 2018, **249**, 457–463.
- 9 Y. J. Chen, H. J. He, H. Y. Liu, H. R. Li, G. M. Zeng, X. Xia and C. P. Yang, Effect of salinity on removal performance and activated sludge characteristics in sequencing batch reactors, *Bioresour. Technol.*, 2018, **249**, 890–899.
- 10 Y. Zhang, Y. Cheng, C. P. Yang, W. Luo, G. M. Zeng and L. Lu, Performance of system consisting of vertical flow trickling filter and horizontal flow multi-soil-layering reactor for treatment of rural wastewater, *Bioresour. Technol.*, 2015, **193**, 424–432.
- 11 W. Luo, C. P. Yang, H. L. He, G. M. Zeng, S. Yan and Y. Cheng, Novel two-stage vertical flow biofilter system for efficient treatment of decentralized domestic wastewater, *Ecol. Eng.*, 2014, **64**, 415–423.
- 12 E. Oguz, Removal of phosphate from aqueous solution with blast furnace slag, *J. Hazard. Mater.*, 2004, **114**, 131–137.
- 13 L. H. Cui, X. Z. Zhu, G. X. Li and B. L. Zhan, Artificial soil rapid infiltration system for treating municipal wastewater in the west of Beijing, China, *Environ. Sci.*, 2000, **20**, 45–48.
- 14 Z. Y. Li, T. B. He, X. M. Yang, C. P. Pan and Z. S. Zhong, Development of constructed rapid infiltration system and its application, *China Water Wastewater*, 2004, **20**, 30–31.
- 15 M. Krol, W. Mozgawa, W. Jastrzebski and K. Barczyk, Application of IR spectra in the studies of zeolites from D4R and D6R structural groups, *Microporous Mesoporous Mater.*, 2012, **156**, 181–188.
- 16 W. Lan, J. Zhang, Z. Hu, M. D. Ji, X. W. Zhang, J. D. Zhang and F. Z. Li, Phosphorus removal enhancement of





- magnesium modified constructed wetland microcosm and its mechanism study, *Chem. Eng. J.*, 2018, **335**, 209–214.
- 17 F. Cavani, F. Trifirò and A. Vaccari, Hydrotalcite-type anionic clays: preparation, properties and applications, *Catal. Today*, 1991, **11**, 173–301.
  - 18 P. S. Braterman, Z. P. Xu and F. Yarberry, Layered metal hydroxides, *Handbook of Layered Materials*, Marcel Dekker, Inc., New York, 2004, pp. 373–474.
  - 19 K. H. Goh, T. T. Lim and Z. Dong, Application of layered double hydroxides for removal of oxyanions: a review, *Water Res.*, 2008, **42**, 1343–1368.
  - 20 K. Hosni and E. Srasra, Evaluation of phosphate removal from water by calcined-LDH synthesized from the dolomite, *Colloid J.*, 2010, **72**, 423–431.
  - 21 K. Teramura, S. J. Iguchi, Y. Mizuno, T. Shishido and T. Tanaka, Photocatalytic conversion of CO<sub>2</sub> in water over layered double hydroxides, *Angew. Chem., Int. Ed.*, 2012, **51**, 8008–8011.
  - 22 R. I. Amann, W. Ludwig and K. H. Schleifer, Phylogenetic identification and *in situ* detection of individual microbial cells without cultivation, *Microbiol. Rev.*, 1995, **59**, 143–169.
  - 23 K. Biswas, M. W. Taylor and S. J. Turner, Successional development of biofilms in moving bed biofilm reactor (MBBR) systems treating municipal wastewater, *Appl. Microbiol. Biotechnol.*, 2013, **98**, 1429–1440.
  - 24 X. L. Zhang, X. T. Liu, L. Xu and J. H. Jin, Purification effect of vertical flow constructed wetlands using modified substrates coated by MgFe-LDHs, China, *Environ. Sci.*, 2013, **33**, 1407–1412.
  - 25 X. L. Zhang, Q. Z. Chen, L. Guo, H. L. Huang and C. Y. Ruan, Effects of varying particle sizes and different types of LDHs-modified anthracite in simulated test columns for phosphorus removal, *Int. J. Environ. Res. Public Health*, 2015, **12**, 6788–6800.
  - 26 X. L. Zhang, L. Guo, H. L. Huang, Y. H. Jiang, M. Li and Y. J. Leng, Removal of phosphorus by the core-shell bio-ceramic/Zn-layered double hydroxides (LDHs) composites for municipal wastewater treatment in constructed rapid infiltration system, *Water Res.*, 2016, **96**, 280–291.
  - 27 X. L. Zhang, Y. Lei, Y. Yuan, J. T. Gao, Y. H. Jiang, Z. Y. Xu and S. J. Zhao, Enhanced removal performance of Cr(VI) by the core-shell zeolites/layered double hydroxides (LDHs) synthesized from different metal compounds in constructed rapid infiltration systems, *Environ. Sci. Pollut. Res.*, 2018, **25**, 9759–9770.
  - 28 C. J. Fang, X. L. Zhang, Y. Lei, Y. Yuan and Y. Xiang, Nitrogen removal via core-shell bio-ceramic/Zn-layer double hydroxides synthesized with different composites for domestic wastewater treatment, *J. Cleaner Prod.*, 2018, **181**, 618–630.
  - 29 SEPA, *Water and wastewater monitoring and analysis method*, China Environmental Science Press, Beijing, 4th edn, 2002.
  - 30 W. J. Weber and J. C. Morris, Kinetics of adsorption on carbon from solution, *J. Sanit. Eng. Div., Am. Soc. Civ. Eng.*, 1963, **89**, 31–60.
  - 31 W. W. Wang, J. B. Zhou, G. Archari, J. G. Yu and W. Q. Cai, Cr(VI) removal from aqueous solutions by hydrothermal synthetic layered double hydroxides: adsorption performance, coexisting anions and regeneration studies, *Colloids Surf., A*, 2014, **457**, 33–40.
  - 32 Y. C. Wang, F. Z. Zhang and S. L. Xu, Preparation of layered double hydroxide microspheres by spray drying, *Ind. Eng. Chem. Res.*, 2008, **47**, 5746–5750.
  - 33 D. G. Evans and R. C. T. Slade, Structural aspects of layered double hydroxides, *Struct. Bonding*, 2006, **119**, 1–87.
  - 34 J. Yu, Q. Wang and D. O'Hare, Preparation of two dimensional layered double hydroxide nanosheets and their application, *Chem. Soc. Rev.*, 2017, **46**, 5950.
  - 35 J. B. Zhou, W. W. Wang, Y. Cheng and Z. Zhang, Facile hydrothermal synthesis and characterization of porous magnesium oxide for parachlorophenol adsorption from the water, *Integr. Ferroelectr.*, 2012, **137**, 18–29.
  - 36 K. Q. Li, Y. Li and Z. Zheng, Kinetics and mechanism studies of *p*-nitroaniline adsorption on activated carbon fibers prepared from cotton stalk by NH<sub>4</sub>H<sub>2</sub>PO<sub>4</sub> activation and subsequent gasification with steam, *J. Hazard. Mater.*, 2010, **178**, 553–559.
  - 37 B. H. Hameed, A. L. Ahmad and K. N. A. Latiff, Adsorption of basic dye (methylene blue) onto activated carbon prepared from rattan sawdust, *Dyes Pigm.*, 2007, **75**, 143–149.
  - 38 M. Wagner and A. Loy, Bacterial community composition and function in sewage treatment systems, *Curr. Opin. Biotechnol.*, 2012, **13**, 218–227.
  - 39 Q. Q. Cao, H. Wang, X. C. Chen, R. Q. Wang and J. Liu, Composition and distribution of microbial communities in natural river wetlands and corresponding constructed wetlands, *Ecol. Eng.*, 2017, **98**, 40–48.
  - 40 G. Ansola, P. Arroyo and L. E. S. Miera, Characterization of the soil bacterial community structure and composition of natural and constructed wetlands, *Sci. Total Environ.*, 2014, **473–474**, 63–71.
  - 41 J. Liu, N. K. Yi, S. Wang, L. J. Lu and X. F. Huang, Impact of plant species on spatial distribution of metabolic potential and functional diversity of microbial communities in a constructed wetland treating aquaculture wastewater, *Ecol. Eng.*, 2016, **94**, 564–573.
  - 42 L. H. Wang, L. Zhang, C. B. Hao, G. C. Wang and P. Shi, Degrading bacteria community structure in groundwater of a petroleum-contaminated site, *Environ. Sci. Technol.*, 2013, **36**, 1–45.
  - 43 C. Kragelund, C. Levantesi, A. Borger, K. Thelen, D. Elkelboom, V. Tandol, Y. Kong, J. Van der Waarde and J. Kroonerman, Identity, abundance and ecophysiology of filamentous Chloroflexi species present in activated sludge treatment plants, *FEMS Microbiol. Ecol.*, 2007, **59**, 671–682.
  - 44 H. Yang, G. Z. Zhang, X. N. Yang, F. P. Wu, W. Zhao, H. W. Zhang and X. Zhang, Microbial community structure and diversity in cellar water by 16S rRNA high-throughput sequencing, *Environ. Sci.*, 2017, **38**, 1704–1715.
  - 45 Y. Özdemir, M. Doğan and M. Alkan, Adsorption of cations dyes from aqueous solutions by sepiolite, *Microporous Mesoporous Mater.*, 2006, **96**, 419–427.
  - 46 B. Yang, D. F. Liu, J. B. Lu, X. R. Meng and Y. Sun, Phosphate uptake behavior and mechanism analysis of facilely



- synthesized nanocrystalline Zn-Fe layered double hydroxide with chloride intercalation, *Surf. Interface Anal.*, 2018, **50**, 378–392.
- 47 A. Halajnia, S. Oustan, N. Najafi, A. R. Khataee and A. Lakzian, Adsorption-desorption characteristics of nitrate, phosphate and sulfate on Mg-Al layered double hydroxide, *Appl. Clay Sci.*, 2013, **80–81**, 305–312.
- 48 T. Shihela and Y. A. Nayaka, Kinetics and thermodynamics of cadmium and lead ions adsorption on NiO nanoparticles, *Chem. Eng. J.*, 2012, **191**, 123–131.
- 49 S. Brown, R. L. Chaney, J. S. Angel and A. J. M. Baker, Phytoremediation potential of *Thlaspi caerulescens* and bladder campion for zinc- and cadmium-contaminated soil, *J. Environ. Qual.*, 1994, **23**, 1151–1157.
- 50 P. R. Qin, M. Xi, J. H. Li, F. L. Kong, Y. Li and J. P. Wang, Effects of phosphorus removal by zeolite modified by Ferric Trichloride, *Wetland Science*, 2017, **15**, 464–469.
- 51 J. P. Liu, X. T. Huang, Y. Y. Li, K. M. Sulierman, X. He and F. L. Sun, Facile and large-scale production of ZnO/Zn-Al layered double hydroxides hierarchical heterostructures, *J. Phys. Chem. B*, 2006, **110**, 21685–21872.
- 52 D. H. Yuan, L. J. Jing, S. X. Gao, D. Q. Yin and L. S. Wang, Analysis on the removal efficiencies of phosphorus in some substrates used in constructed wetland systems, *Environ. Sci.*, 2005, **26**, 51–55.
- 53 X. H. Yi, D. D. Jing, J. Wan, Y. Ma and Y. Wang, Temporal and spatial of contaminant removal, enzyme activities, and microbial community structure in a pilot horizontal subsurface flow constructed wetland purifying industrial runoff, *Environ. Sci. Pollut. Res.*, 2016, **23**, 8565–8576.

